ARTICLE

Engineering *Pseudomonas putida* for improved utilization of syringyl aromatics

Joshua Mueller[1] | Howard Willett[1] | Adam M. Feist[3,4] | Wei Niu[1,2]

[1]Department of Chemical and Biomolecular Engineering, University of Nebraska-Lincoln, Lincoln, Nebraska, USA

[2]The Nebraska Center for Integrated Biomolecular Communication (NCIBC), University of Nebraska-Lincoln, Lincoln, Nebraska, USA

[3]Department of Bioengineering, University of California, San Diego, California, USA

[4]Novo Nordisk Foundation Center for Biosustainability, Technical University of Denmark, Lyngby, Denmark

Correspondence

Wei Niu, Department of Chemical and Biomolecular Engineering, University of Nebraska-Lincoln, Lincoln, NE 68588, USA.
Email: wniu2@unl.edu

Abstract

Lignin is a largely untapped source for the bioproduction of value-added chemicals. *Pseudomonas putida* KT2440 has emerged as a strong candidate for bioprocessing of lignin feedstocks due to its resistance to several industrial solvents, broad metabolic capabilities, and genetic amenability. Here we demonstrate the engineering of *P. putida* for the ability to metabolize syringic acid, one of the major products that comes from the breakdown of the syringyl component of lignin. The rational design was first applied for the construction of strain Sy-1 by overexpressing a native vanillate demethylase. Subsequent adaptive laboratory evolution (ALE) led to the generation of mutations that achieved robust growth on syringic acid as a sole carbon source. The best mutant showed a 30% increase in the growth rate over the original engineered strain. Genomic sequencing revealed multiple mutations repeated in separate evolved replicates. Reverse engineering of mutations identified in *agmR*, *gbdR*, *fleQ*, and the intergenic region of *gstB* and *yadG* into the parental strain recaptured the improved growth of the evolved strains to varied extent. These findings thus reveal the ability of *P. putida* to utilize lignin more fully as a feedstock and make it a more economically viable chassis for chemical production.

KEYWORDS

adaptive lab evolution (ALE), *Pseudomonas putida* KT2440, syringyl lignin-derived aromatics

1 | INTRODUCTION

Lignin is a complex organic polymer that makes up 20%–35% of plant cell walls. It is polymerized from three monolignols: *p*-coumaryl alcohol, coniferyl alcohol, and sinapyl alcohol, which are categorized as the corresponding hydroxy (H), guaiacyl (G), and syringyl (S) lignin components (Figure 1a; Feofilova & Mysyakina, 2016). Depending on the type of plants, the ratio of H, G, and S subunits in lignin varies, where the grass lignin consists of all subunits, the softwood lignin often has low S component (Gellerstedt & Henriksson, 2008). The heterogeneity of lignin makes it a difficult target for traditional catalytic and enzymatic refinement approaches (C. Li et al., 2015; Rinaldi et al., 2016; Schutyser et al., 2018; Sun et al., 2018; Zakzeski et al., 2010). As a result, most lignin streams generated in existing processing facilities are burned as a low-grade fuel (Ragauskas et al., 2014). Recent development in the biofuel technology, in particular the potential use of lignocellulosics as the starting material, ignites research interests into the valorization of lignin streams through microbial conversions of its degradation products (Becker & Wittmann, 2019; Eltis & Singh, 2018; Linger et al., 2014). Breakdowns of lignin can lead to an assortment of compounds that
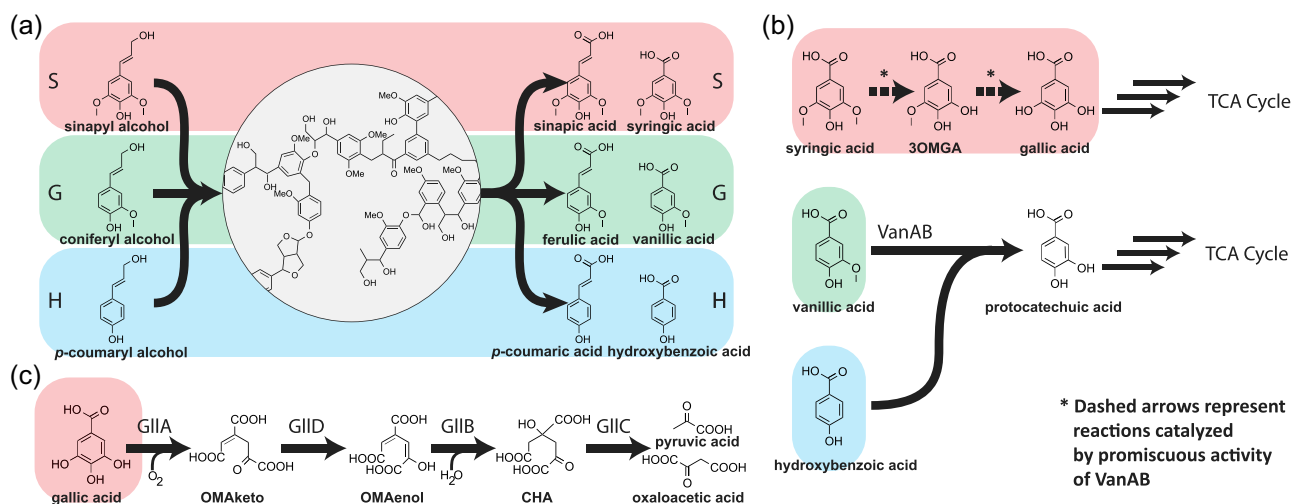
FIGURE 1 Lignin synthesis and degradation pathways. (a) Schematics for the polymerization of monolignols (left) into polymeric lignin (center) followed by its depolymerization into model monomeric aromatic products (right). (b) Catabolic pathways of model depolymerization products in *P. putida*. The known reaction catalyzed by VanAB is marked with solid arrows. Potential reactions for the conversion of syringic acid into gallic acid using VanAB are shown using dashed arrows. (c) The native *P. putida* catabolic pathway for gallic acid through the intermediates, including 4-oxalomesaconic acid (OMA) keto and enol forms, and 4-carboxy-4-hydroxy-2-oxoadipic acid (CHA). Enzymes, gallic acid dioxygenase (GllA), OMA keto–enol tautomerase (GllD), OMAenol hydratase (GllB), and CHA aldolase (GllC).

preserve the core chemical structures of the three monolignols. Maximizing the value of lignin therefore calls for a complete utilization of all components in the lignin depolymerization mixture.

Several microorganisms, such as *Pseudomonas putida* (Salvachúa et al., 2020; Willett, 2019), *Sphingobium* sp. SYK-6 (Araki et al., 2020; Gall et al., 2014; Meux et al., 2012; Sato et al., 2009), and *Novosphingobium aromaticivorans* (Bell et al., 2012; Cecil et al., 2018; Kontur et al., 2018; Perez et al., 2019, 2020), are being investigated for their abilities to utilize lignin-derived compounds. Among them, *P. putida* KT2440 has emerged as a suitable candidate for industrial bioprocessing of lignin due to its genetic tractability, high tolerance to industrial solvents, and readily available engineering tools (Martínez-García & de Lorenzo, 2019; Nikel & de Lorenzo, 2018). KT2440 can utilize a large number of carbon substrates, including compounds obtained from the breakdown of lignin (Dos Santos et al., 2004; Nikel & de Lorenzo, 2018; Nikel et al., 2014). It encodes pathways to metabolize vanillate, ferulate, *p*-coumarate, and 4-hydroxybenzoate which are the major degradation products from the G and H components of lignin (Harwood & Parales, 1996; Jiménez et al., 2002; Nogales et al., 2017) (Figure 1a,b). Notably, it lacks the ability to use syringate or sinapate as a sole carbon source, which are compounds derived from the lignin's syringyl components (Figure 1a,b). Successful engineering of S lignin metabolism in the KT2440 strain therefore will greatly boost its application in lignin valorization.

In this report, we demonstrate the successful engineering of syringate metabolism in KT2440 through a combined approach of chromosomal overexpression of the vanillate demethylase (VanAB) and subsequent adaptive lab evolution (ALE). Experimental analysis of mutations identified in the ALE mutants provided insights into potential causal genetic and metabolic changes that led to the improved growth on syringate.

2 | MATERIALS AND METHODS

2.1 | Media and cultivation methods

All commercial chemicals are of reagent grade or higher. All solutions were prepared in deionized water that was further treated by the Barnstead Nanopure® ultrapure water purification system (Thermo Fisher Scientific Inc.). Preparation of LB media and M9 salts followed reported recipe (Niu et al., 2019). M9 media contained $MgSO_4$ (0.12 g/L), $CaCl_2$ (0.028 g/L), and trace metal solution (Studier, 2005). Kanamycin was included in the media at 50 mg/L when it was needed. Solutions of M9 salts, glucose, $MgSO_4$, and $CaCl_2$ were autoclaved separately and then mixed. M9 media was used for growth testing. The media was supplemented with 0.25% (w/v) vanillic acid or 0.2% (w/v) syringic acid. The pH values of all minimal media were adjusted to 7.0. Media containing syringic acid was also supplemented with cysteine (6 mM) to prevent its oxidation. All cell culture experiments were conducted at 30°C under the shake flask condition with agitation at 250 rpm. For growth tests, a seed culture was started by inoculating LB media with a single colony from a freshly streaked LB agar plate. Following overnight cultivation, 1 mL cells were collected by centrifugation, washed, then resuspended in an equal volume of M9 salts. Cell densities were determined by measurement of absorbance at 600 nm (OD_{600}) using a Synergy HTX Multi-Mode Reader. Appropriate volumes were introduced into 5 ml of fresh M9 media containing a desired carbon source to reach an initial OD_{600} of 0.05. Cells were cultured in a 36-ml glass culture

tube. Cell growth was monitored by taking OD measurements at indicated times. Triplicate cultures were included in each growth experiment.

2.2 | Strains and plasmids

The wild-type *Pseudomonas putida* KT2440 was obtained from the American Type Culture Collection (ATCC 47054). *Escherichia coli* NEB® 5-alpha (New England Biolabs) was used as the host in molecular cloning experiments. Standard protocols were used for the construction, purification, and analysis of plasmid DNA (Sambrook & Russell, 2000). Bacterial genomic DNAs were isolated using the PureLink™ genomic DNA mini kit (Thermo Fisher Scientific). PCR amplifications were carried out using KOD Hot Start or KOD Xtreme™ Hot Start DNA polymerase (Millipore Sigma) by following the manufacturer's protocol. Other molecular cloning reagents were purchased from New England Biolabs. Primer synthesis and Sanger sequencing services were provided by Eurofins MWG Operon. Bacterial strains and plasmids used and constructed in this study are listed in Table 1. Primers used in this study are listed in Supporting Information: Table S1. Plasmids were constructed using the Sequence and Ligation Independent Cloning (SLIC) protocol (M. Z. Li & Elledge, 2012). Plasmids for the chromosomal modification of KT2440 were derived from pK19mobsacB, which is nonreplicable in KT2440 (Simon et al., 1983). For the integration of the P$_{lac}$ promoter, two 0.5-kb DNA fragments that are homologous to either the upstream or the downstream sequences of the *vanAB* insertion site were first ligated into the *Hind*III and *Pst*I sites of pK19mobsacB. A DNA fragment encoding

the P$_{lac}$ promoter was subsequently cloned between the two homology fragments. The plasmid used for the deletion of *PP_3350* gene was constructed by ligating two 0.5-kb fragments flanking the target gene into pK19mobsacB. To introduce single-nucleotide polymorphism (SNP) mutations identified in the *agmR*, *fleQ*, *gbdR*, or *gstB-yadG* genes, 1 kb DNA fragments that covered the mutation site were amplified from the genome of ALE mutants, then cloned into pK19mobsacB. Chromosome modification started with the electroporation of plasmid DNA into a KT2440 host. Electrocompetent KT2440 cells were prepared following published protocols (Choi et al., 2006). Successful plasmid insertion clones were selected on LB plates containing kanamycin. Successful removal of the plasmid backbone from the chromosome was identified using the SacB-mediated counter selection method (Schäfer et al., 1994). Chromosomal modifications were confirmed by DNA sequencing.

2.3 | Analysis methods

Samples for metabolite analysis were collected from cell culture, and then centrifuged at 21,000 g for 5 min. The supernatant was combined with D_2O with the sodium salt of 3-(trimethylsilyl) propionic-2,2,3,3-d$_4$ acid (TSP) at 9:1 (v/v) ratio. All ^1H NMR spectra were recorded on a Bruker Avance III-HD NMR Spectrometer (300 MHz). A solvent suppression program was applied to suppress the signal of water. Concentrations were determined by comparison of integrals corresponding to each compound with the integral corresponding to TSP ($\delta = 0.00$ ppm). A standard concentration curve was determined for each metabolite of interest. Compounds were quantified by using the following resonance signals: syringic acid

TABLE 1 Strains and plasmids used in this study.

	Strains/plasmid	Characteristics	Source
1	*P. putida* KT2440	Wild type	ATCC 47054
2	*P. putida* Sy-1	KT2440, P$_{lac}$P$_{vanA}$	This study
3	*P. putida* Sy-1 gbdR-SNP	KT2440 Sy-1 *gbdR* S197A T > G	This study
4	*P. putida* Sy-1 fleQ-SNP	KT2440 Sy-1 *fleQ* R355P C > G	This study
5	*P. putida* Sy-1 gstB-SNP	KT2440 Sy-1 *gstB* + 58 C > T	This study
6	*P. putida* Sy-1 agmR-SNP	KT2440 Sy-1 *agmR* I81T A > G	This study
7	*P. putida* Sy-1 ΔPP_3350	KT2440 Sy-1 ΔPP_3350	This study
8	*E. coli* NEB 5α	cloning host	NEB
9	pK19mobsacB	Kan^R, chromosomal modification vector	ATCC 87098
10	pK19mobsacB-P$_{vanA}$-P$_{lac}$-vanA	Kan^R, P$_{lac}$ insertion upstream of *vanAB*	This study
11	pK19mobsacB-ΔPP_3350	Kan^R, deletion of *PP_3350*	This study
12	pK19mobsacB-gbdR-SNP	Kan^R, *gbdR* S197A T > G	This study
13	pK19mobsacB-fleQ-SNP	Kan^R, *fleQ* R355P C > G	This study
14	pK19mobsacB-gstB-SNP	Kan^R, *gstB* + 58 C > T	This study
15	pK19mobsacB-agmR-SNP	Kan^R, *agmR* I81T A > G	This study

(δ 7.28, s, 1H), 3-*O*-methyl gallic acid (δ 7.14, dd, 1H), and gallic acid (δ 7.05, dd, 1H).

Gene expression levels were determined using quantitative PCR (qPCR) following the previously reported protocol (Willett, 2019). Total RNA was isolated from cells that were cultured in M9 media with the desired carbon source. Primers for qPCR (Supporting Information: Table S1) were designed using the Primer3Plus program with targeted amplicons of around 100 bp. Efficiencies of PCR reactions were determined to be 96%–99% using standard curve analysis. Single melting peaks were observed for all PCR reactions. The qPCR data were processed using CFX Manager Software (Bio-Rad). Changes in the expression level of a target gene were calculated using the $2^{-\Delta\Delta Ct}$ method. The expression level of the *dnaA* gene, which encodes the chromosomal replication initiator protein, was used as the reference.

2.4 | Adaptive laboratory evolution (ALE) and mutation analysis

An overnight seed culture of the Sy-1 strain in LB media was collected by centrifugation, then washed and resuspended in an equal volume of M9 salt media. ALE experiments were initiated by starting three replicate cultures from the starting seed culture into 5 ml of M9 media containing syringate as the sole carbon source at an initial OD of 0.1. Cell cultivation followed the general protocol in 2.1. Cell growth was monitored daily until the OD was greater than 1. Each independent replicate evolution was then diluted into 5 ml fresh M9 syringate media for continued culturing. The growth rate assumed constant exponential growth for each passage, or flask, and was calculated using a standard logarithmic growth rate where the natural logarithm of the final OD divided by the starting OD of each flask was divided by the time between each passage (Figure 3). The serial subculturing step was repeated until the cell growth reached an OD of 1 in less than 24 h at which point the ALE experiments were terminated. Glycerol stocks were prepared at each subculturing step.

Upon completion of the ALE experiment, single colonies were isolated by plating the ALE culture on LB agar. Individual colonies were then tested for growth on syringate as the sole carbon source. For mutation analysis, genomic DNA from strains of interest were isolated. Genome sequencing services using Illumina MiSeq™ system were provided by GENEWIZ. The average coverage for each sample was over 60×. The sequencing files were analyzed using a previously described script (Phaneuf et al., 2019) based on bowties2 (Deatherage & Barrick, 2014). The NCBI NC_002947 version 4 reference genome for *P. putida* KT2440 (www.ncbi.nlm.nih.gov/nuccore/NC_002947.4/) was used for annotation of genes. For population samples, a filter was applied to exclude mutations with a frequency of less than 0.50, unless the same mutation was found in an isolate. This value was selected to focus on likely causal mutations which enriched during the ALE experiments. The resultant information was hosted on ALEdb (Phaneuf et al., 2019) and used to identify potential mutations of interest.

3 | RESULTS

3.1 | Engineering syringate metabolism in KT2440

Although the wild-type KT2440 strain lacks the ability to grow solely on syringate, it encodes enzymes for the metabolism of its double demethylation product, gallate (Figure 1c). A KT2440 mutant, which expresses a functional gallate transport protein (GllT) due to a single nucleotide deletion, was reported previously for its ability to use gallate as a carbon source (Nogales et al., 2011). In our preliminary studies, we demonstrated that the vanillate demethylase of KT2440 (encoded by *vanAB*) was capable of catalyzing the demethylation of both meta methoxy groups in syringate (Figure 1b; Willett, 2019). We observed the conversion of syringate and 3-*O*-methyl-gallate, the single demethylation product of syringate, into gallate by *E. coli* cells that expressed the KT2440 VanAB protein (Willett, 2019). Wild-type KT2440 that overexpressed VanAB from a plasmid also consumed syringate as a carbon source, albeit requiring the presence of glucose for growth (Willett, 2019). The observed catalytic promiscuity of the vanillate demethylase from KT2440 towards syringate was also reported recently (Notonier et al., 2021).

We hypothesized that the inability of the VanAB-overexpressing strain to use syringate as the sole carbon source is caused by the metabolic burden of high-level protein expression and plasmid maintenance. To achieve a reduced and stable expression of VanAB, a P_{lac} promoter was inserted between the native promoter of the *vanAB* gene cluster (P_{vanAB}) and the open reading frame of the *vanA* gene (Figure 2a). Since the native P_{vanAB} is repressed by its transcriptional repressor (VanR), which is alleviated in the presence of vanillate, the genetic insertion led to the constitutive expression of the VanAB protein. qPCR analysis of the expression level of *vanA* gene in the Sy-1 and the wild-type KT2440 strains validated the design (Figure 2b). A vanillate-independent transcription of *vanA* was observed in Sy-1 strain cultured on glucose as the transcript level was higher than when the wild-type KT2440 was cultured on vanillate, presumably because the P_{lac} is stronger than the native P_{vanAB} promoter (Figure 2b). Further increase in the transcription of *vanA* when Sy-1 strain was cultured on vanillate indicated an additive effect of the two promoter sequences (Figure 2b).

The Sy-1 strain was further characterized in M9 media containing glucose, vanillate, or syringate as the sole carbon source (Figure 2c). Sy-1 showed robust growth with a rate of $0.088 \pm 0.032\,h^{-1}$ when syringate was provided, while no growth was detected for the wild-type KT2440 strain following 96 h of cultivation. The constitutive expression of the VanAB protein under a stronger promoter also led to a shorter lag phase and higher cell density of the Sy-1 strain cultured on vanillate. Meanwhile, the chromosomal modification did not cause substantial growth change between the Sy-1 and the wild-type strain when glucose was the carbon source. Measurements of syringate concentrations also showed that VanAB overexpression allowed *P. putida* to metabolize syringate over a period of 96 h and that the rate of consumption was higher when vanillic acid was

present (Figure 2d), which would be expected due to the higher expression levels from both the P$_{lac}$ and P$_{vanA}$ promoters. An elevated expression of genes in gallate operons, that is, *gllA* and *gllB*, were detected (Supporting Information: Figue S1) as a result of induced expression by gallate, which is a metabolic intermediate of syringate (Figure 1c). However, accumulation of gallate and another metabolic intermediate, that is, 3-O-methyl-gallate, was not detected.

3.2 | Adaptive lab evolution of the Sy-1 strain on syringate utilization

The Sy-1 strain displayed a long lag phase of nearly 24 h and slow growth rate when cultured on syringate. To improve its growth

characteristics, an ALE experiment was set-up in M9 media with syringate as the sole carbon source in three independent evolution replicates. The experiment was designed to apply a selective pressure for mutations that benefit cells' growth rate on syringate. Due to the extended lag phase and slow growth rate of the Sy-1 strain, initial passages were infrequent and large-volume inoculations (1/6th of the total culture) were carried out each time. As growth characteristics improved, the passage volume was eventually decreased to 2% of the total volume. To gauge the progress of the evolution, average growth rates were estimated using the starting OD, ending OD, time interval of each passage, and the assumption of continued exponential growth. A continuous improvement over time was observed throughout the ALE experiment (Figure 3). After 105 days of ALE, the average growth rate reached approximately 2.8 day^{-1}, which was a
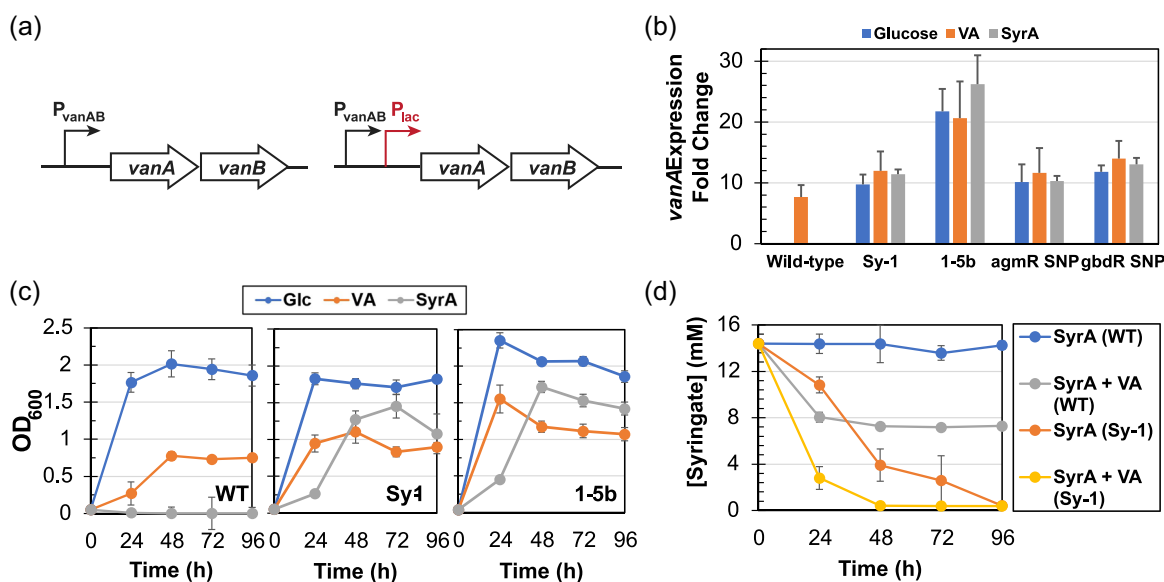
FIGURE 2 Construction and characterization of Sy-1 and evolved strains. (a) Chromosomal insertion of the P$_{lac}$ promoter. (b) qPCR analysis of *vanA* expression normalized to expression level of *vanA* in wild-type *P. putida* grown in glucose. (c) Growth characterization of wild-type, Sy-1, and 1-5b strains on glucose (Glc), vanillate (VA), and syringate (SyrA). (d) Concentration change of syringate over time in culture media of wild type or Sy-1 strain. (b–d) Results are represented as the average values of triplicate with standard deviations.
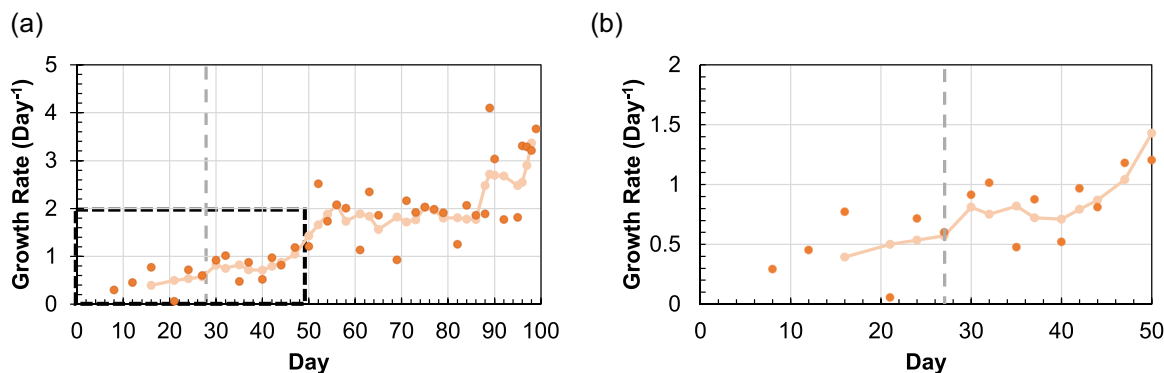
FIGURE 3 Average growth rates of adaptive laboratory evolution cultures. (a) Full experiment duration of 100 days. (b) Focused view of first 50 days. Darker dots show growth rates of each passage whereas the lighter line is the moving average of the three previous passages. The timepoint used for sequencing of samples from the early stage of the ALE experiment is denoted by the dashed gray line.

sevenfold improvement in comparison to the values observed at the beginning of the experiment. Upon completion of the ALE, single colonies were isolated from each of the three independent experiments. Five isolates from each endpoint population of the three replicates were characterized for growth on syringate as the sole carbon source (growth data of the isolate with the fastest growth rate from each replicate culture are included in the Supporting Information). All evolved strains showed significantly improved growth characteristics, including duration of lag phase and growth rate, compared to the parental Sy-1 strain. Isolates with the greatest improvements showed reduced lag times of approximately 20 h, improved growth rates, and higher maximum ODs of 1.3–1.8 in comparison to a maximum OD of 0.95 for the Sy-1 strain.

3.3 | Genomic and genetic analysis of ALE mutants

Genomic sequencing analysis allowed for the identification of key mutations that led to improved growth. Sequencing was conducted on 13 samples, including isolated strains and mixed populations. In addition to the parent strain, Sy-1, one isolate with an improved growth rate was selected from each independent replicate on Day 27 and at the end of the ALE experiments to reveal the mutations associated with the improved growth phenotype. ALE population samples of each experiment were also analyzed from the 27th and final day to provide insights into the relative frequency of specific mutations at that point in evolutionary time. The genomes from the earlier stages of the experiment also allowed for identifying any mutations that increased or fixed in allelic frequency. The genome of the Sy-1 strain was first used as the reference to identify sequence differences from the published genome of wild-type KT2440 in NCBI. These differences are potential mutations that occurred before the ALE experiment and were excluded from the analysis. After filtering out 26 mutations found in the Sy-1 strain, a total of 82 unique mutations either were identified in the six isolates or appeared in more than 50% of reads from one of the six population samples (Supporting Information: Table S2). The majority (45 mutations) were single-nucleotide polymorphisms (SNPs), roughly a quarter were either deletion (17) or insertion (19) mutations, and one mutation was a multiple-base substitution. No mutation was observed in the upstream regulatory region or within the vanAB genes. These unique mutations were observed a total of 250 times across all samples with several mutations occurring multiple times. One group of the repeated mutations appeared in the midpoint and the corresponding end-point populations, which indicated a continued presence of early mutations in the population sample. Another group of repeated mutations was observed in both isolated clones and in the corresponding ALE population sample, which indicated the isolates were representative of the source culture. More importantly, the third group of repeated mutations was found across two or more population replicates. These convergent mutations, which occurred in gbdR, yiaY, fleQ, and the intergenic region between gstB and yadG (Supporting Information: Table S3), indicated a strong possibility of evolutionary benefits under the selective pressures that were applied. A few mutations were identified in genes that were reported to have high mutational frequency in others' ALE experiments. This includes the flagellar genes fleQ and fliF (Supporting Information: Table S2).

To further deconvolute the effect of individual mutations on the growth improvement of ALE mutants, we introduced several selected observed mutations individually into the parent strain, Sy-1. ALE mutant Sy-1 1-5b, which was isolated from the final flask of replicate 1, showed reduced lag time and significantly improved growth rate on syringate without the accumulation of gallate and 3-O-methylgallate. Strain 1-5b also had similar growth characteristics on glucose as the parent, but increased OD when cultured on vanillate (Figure 2c). qPCR analysis of the strain showed a 129% increase in the expression level (p value: 5.77×10^{-3}) of the vanA gene in comparison to Sy-1 when grown on syringic acid (Figure 2b). An elevated expression level of the gallate-metabolizing genes was also observed. As downstream steps in the assembled metabolic pathway of syringate, the increased mRNA levels of the enzymes likely corresponded to higher flux through the pathway and increased growth rate (Supporting Information: Figure S1). Genomic sequencing of Sy-1 1-5b strain revealed four mutations, including SNPs in genes agmR, gbdR, and fleQ, as well as in the intergenic region between gstB and yadG. The agmR SNP was observed in the mid-point population of replicate 1 at a frequency of 9.3% of the reads. By the final flask of the ALE, this mutation occurred in 85% of the reads. The mutations in the gbdR gene and the gstB-yadG intergenic region were also observed in the population sample from Replicate 3 and its corresponding endpoint isolate. In addition to above mutations observed in Sy-1 1-5b, we examined the deletion of gene PP_3350, which was identified in a previous ALE study to benefit the growth of KT2440 on p-coumaric acid, a degradation product of the H lignin (Mohamed et al., 2020).

After incorporating individual mutations identified from the ALE experiment into the Sy-1 strain, obtained mutants were examined for growth in minimal media containing only syringate (Figure 4). The strain with an SNP in agmR showed the greatest improvement when the average growth rate was considered (Table 2). However, this change is not statistically significant ($p > 0.05$) when comparing to the growth rate of the parent strain Sy-1. The gbdR, fleQ, and yadG-gstB strains showed a modest improvement in growth, but a noticeable increase in maximum OD as shown in Figure 4a,b. The consumption of syringate was only increased slightly in the fleQ strain as shown in Figure 4d. Deletion of the PP_3350 gene did not result in substantial improvement in growth or syringate utilization in comparison to the parent Sy-1 strain. qPCR analysis of vanA gene and gallate-metabolizing genes were conducted in strains with mutations in agmR or gbdR gene, which encode possible transcriptional regulators. Expression levels similar to those in the Sy-1 parent strain were observed under all cultivation conditions (Figure 2b and Supporting Information: Figure S1).
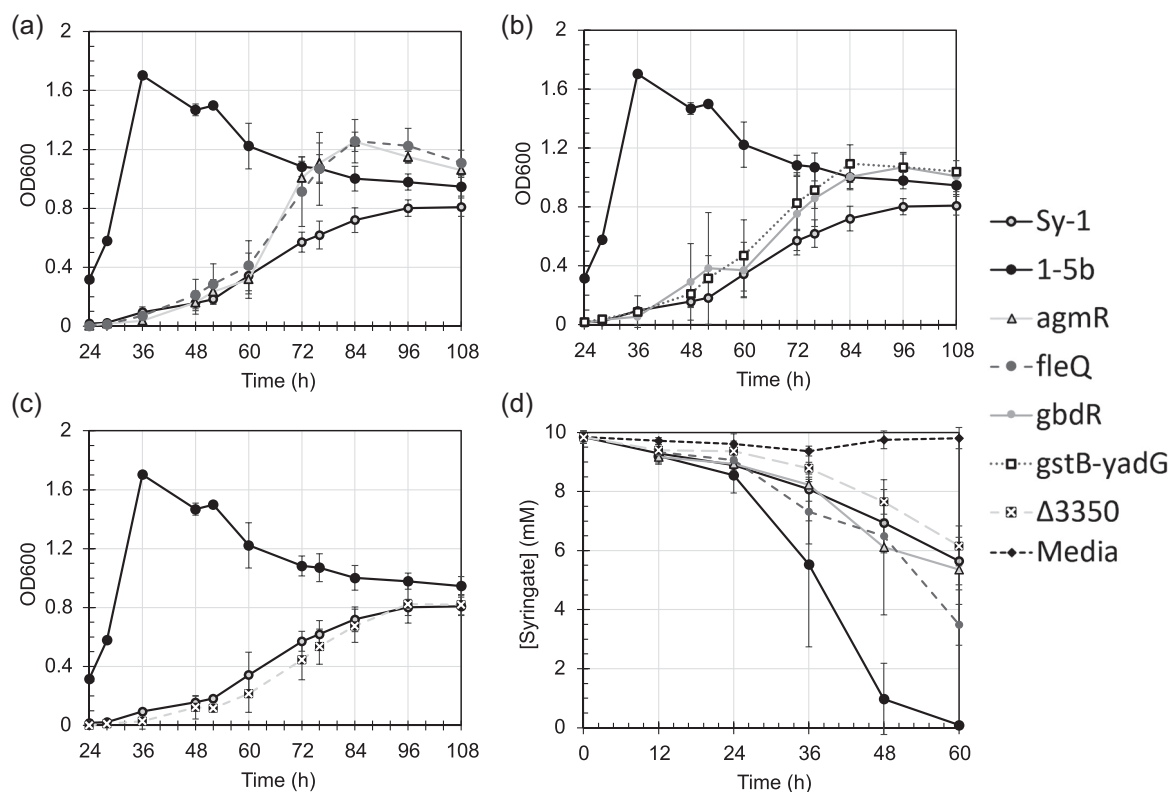
FIGURE 4 Characterization of Sy-1 mutants on the utilization of syringic acid. (a–c) Comparing the growth of modified Sy-1 strains with the growth of Sy-1 and evolved 1-5b strain. (a) *agmR* and *fleQ* mutants. (b) *gbdR* and *gstB-yadG* mutants. (c) ΔPP_3350 mutant. (d) Consumption of syringate over time by all strains.

TABLE 2 Growth rates of Sy-1 and derivatives on syringic acid.

Strain/Modification	Growth rate (h^{-1})
Sy-1	0.088 ± 0.032
1-5b	0.115 ± 0.035
gbdR	0.096 ± 0.019
agmR	0.110 ± 0.019
gstB-yadG	0.096 ± 0.032
fleQ	0.094 ± 0.041
ΔPP_3350	0.054 ± 0.009

4 | DISCUSSION

P. putida is a promising bacterial chassis for the production of value-added chemicals from lignin depolymerization compounds (Martínez-García & de Lorenzo, 2019; Nikel & de Lorenzo, 2018; Nikel et al., 2016). Here, we demonstrated the successful engineering of *P. putida* KT2440 for growth on syringic acid by first overexpressing the native *vanAB* genes in strain Sy-1 followed by its ALE experiment with syringic acid as the sole carbon source. ALE has been used to identify novel approaches to solve complex engineering problems in *P. putida*, including to enhance tolerance to toxic compounds, such as anthranilate (Kuepper et al., 2020), ionic liquids (Lim et al., 2020),

solvents (Kusumawardhani et al., 2021), and lignin-derived acids (Mohamed et al., 2020), and to improve the efficiency of catabolic pathways for ethylene glycol, 1,4-butanediol (W.-J. Li et al., 2020; W. J. Li et al., 2019), and xylose (Lim et al., 2021). Our ALE process spanned over 3 months to improve an average growth rate of the ALE culture from 0.4 to 2.8 day^{-1}, which is a combined result of shortened lag phase and increased growth rate. One of the best evolved mutant Sy-1 1-5b has a lag phase of 8 h and a growth rate of 0.115 h^{-1}, an 83.3% reduction, and 34.1% improvement, respectively.

Genome sequencing data of ALE population and ALE isolates with improved growth revealed a plethora of genetic changes in the dynamic evolution process. We took a combined approach of literature searching and experimental verification to identify mutations that could contribute to the improved fitness of Sy-1 mutants in media with syringate. Among unique mutations, certain ones emerged at the early stage of the ALE process but did not further prevail. For example, a total of eight unique SNPs were observed in gene *PP_0168* (Supporting Information: Table S2), which encodes a possible surface adhesion protein. Since the formation of biofilm is a commonly observed microbial behavior in suspension cultures, such mutations were hypothesized as neutral drift, which are irrelevant to the evolutionary pressure. Mutations in *fleQ* (three unique mutations) and *fliF* (two unique mutations) (Supporting Information: Table S2) have been previously identified as common mutation targets in ALE experiments. It was hypothesized that the reduced or loss of ability to

express flagellar saves energy from producing an unnecessary cell organelle under the shake flask environment. Strains of *P. putida* have been previously generated lacking the majority of flagellar genes which results in enhanced energy metabolism (Martínez-García et al., 2014; Mohamed et al., 2020). We also observed a large number of mutations that occurred in intergenic regions and a small number of SNPs in uncharacterized genes. Further rationalization of these mutations is challenging due to the lack of gene(-protein) knowledge. We then proceeded with an approach of directly analyzing mutations in an ALE isolate with known improved growth on syringate.

The three genomically sequenced ALE isolates had 4 (1-5b), 10 (2-5a), and 8 (3-5d) mutations, respectively (Supporting Information: Table S2). We retrofitted individual mutations from 1 to 5b into the Sy-1 strain and observed between a 9% and 25% improvement in growth rate along with increased biomass accumulation (Table 2 and Figure 4). Of the four mutations tested, the *agmR* SNP had the greatest impact on growth, including the highest growth rate and one of the highest maximum OD. The mutation was also found in 85.1% of the sequenced DNA in the final ALE culture of Replicate 1, indicating that it was favorably propagated under the selective pressure. The *agmR* gene encodes a LuxR family transcriptional regulator. As a relatively understudied protein, limited literature showed that AgmR may play a role in regulating the expression of coenzyme PQQ synthesis protein A (PqqA) and ABC transport genes PP_2667 and PP_2669 (Vrionis et al., 2002). PQQ is a key component in bacterial redox metabolism, and often acts as a cofactor in alcohol dehydrogenases. Changes in the intracellular level of PQQ may lead to the change in cellular redox state, which was shown to be an important factor in the bacterial metabolism of aromatic compounds (Henson et al., 2018). The ABC transport system encoded by PP_2267-PP_2269 was hypothesized to function in the uptake of 2-phenylethanol based on their essentiality for growth (Wehrmann et al., 2019). Structural similarity between 2-phenylethanol and syringate indicates possible cross-activity towards syringate as the substrate. Both the biosynthesis of PQQ and a potential ABC transporter are relevant to syringate utilization and changes in their expression level could lead to the phenotypic change of the Sy-1 agmR-SNP strain. Introduction of the other three mutations in Sy-1 led to similar changes in growth characteristics on syringate. A possible role in improving cells' energy metabolism (Martínez-García et al., 2014) by the *fleQ* SNP is discussed above. Two additional *fleQ* mutations were observed in the final ALE culture and the isolate of Replicate 2. The *gbdR* SNP identified in 1-5b was found as a dominant mutation in the final ALE culture of both Replicate 1 (90.2%) and Replicate 3 (90.5%). In addition, two other mutations in the *gbdR* gene were observed in the final ALE culture and the isolate of replicate 2. The high mutation frequency in *gbdR* indicates its possible role in regulating cellular function(s) that is relevant to syringate metabolism. As a transcriptional activator, the GbdR in *P. aeruginosa* activates the transcription of the *cbcXWV* gene cluster, which encodes a primary ABC transporter of choline (Malek et al., 2011; Wargo, 2013). The SNP at the intergenic region of the *gstB* and *yadG* genes in strain 1-5b was also observed in the final ALE culture and the isolate of Replicate 3. It is possible that the mutation, which is upstream of the *yadG*, affects the expression level of this transporter protein. Although implied with transport-related function, a direct link between the *gbdR* SNP, the *gstB-yadG* SNP, and syringate catabolism requires further investigations.

All four Sy-1 strains with a single mutation from 1 to 5b demonstrated improved growth on syringate, but none of them reproduced the characteristics of the 1-5b strain. In particular, an increased expression level of the *vanA* gene was observed in 1-5b, but not in the reverse-engineered strains (Figure 2b). The results indicate that every mutation confers benefits to a limited extent. The drastic improvement observed in 1-5b is likely due to additive or synergistic effects of mutations in multiple genes. A larger number of mutations were identified in isolates 2-5a and 3-5d from ALE Replicates 2 and 3, respectively. Besides sharing a few gene targets of mutation, the majority of the mutation sites in these two strains are not presented in strain 1-5b. Further deconvoluting the genetic cause(s) of their phenotypic change is more challenging. The observation showed us that this engineering problem potentially has multiple solutions, which cannot be easily envisioned through a rational approach.

5 | CONCLUSIONS AND FUTURE WORK

In this study, we successfully engineered *P. putida* KT2440 derivatives for robust growth using syringate as the sole carbon source through a combined approach of rational strain design and adaptive lab evolution. Genome sequencing and genetic analysis revealed a few mutations that enhanced the strain's fitness. To better understand how each mutation alters cellular states, we currently are conducting omics studies, in particular transcriptomics and targeted proteomics. Meanwhile, improvement in the growth characteristics of the best mutant, 1-5b, may be achieved through another round of combined efforts of rational design and ALE experiments in light of results from the omics studies. Lignin is an attractive carbon source for bioproduction due to the projected large volume from biofuel production. The efficient use of lignin plays a critical role in the bioeconomy. Our work reported here provides a solid basis for further strain improvements of *P. putida* KT2440, a promising chassis of bio-industrial applications for lignin valorization.

ACKNOWLEDGMENTS

CONFLICTS OF INTEREST

The authors declare no conflicts of interest.

DATA AVAILABILITY STATEMENT

The data that support the findings of this study are available from the corresponding author upon reasonable request.

ORCID

Joshua Mueller http://orcid.org/0000-0001-9092-1222
Adam M. Feist http://orcid.org/0000-0002-8630-4800
Wei Niu http://orcid.org/0000-0003-3826-1276

REFERENCES

Araki, T., Tanatani, K., Kamimura, N., Otsuka, Y., Yamaguchi, M., Nakamura, M., & Masai, E. (2020). The syringate O-demethylase gene of Sphingobium sp. strain SYK-6 is regulated by DesX, while other vanillate and syringate catabolism genes are regulated by DesR. *Applied and Environmental Microbiology*, 86(22), e01712–e01720.

Becker, J., & Wittmann, C. (2019). A field of dreams: Lignin valorization into chemicals, materials, fuels, and health-care products. *Biotechnology Advances*, 37(6), 107360. https://doi.org/10.1016/j.biotechadv.2019.02.016

Bell, S. G., Yang, W., Yorke, J. A., Zhou, W., Wang, H., Harmer, J., Copley, R., Zhang, A., Zhou, R., Bartlam, M., Rao, Z., & Wong, L. L. (2012). Structure and function of CYP108D1 from *Novosphingobium aromaticivorans* DSM12444: An aromatic hydrocarbon-binding P450 enzyme. *Acta Crystallographica. Section D: Biological Crystallography*, 68(3), 277–291.

Cecil, J. H., Garcia, D. C., Giannone, R. J., & Michener, J. K. (2018). Rapid, parallel identification of catabolism pathways of lignin-derived aromatic compounds in *Novosphingobium aromaticivorans*. *Applied and Environmental Microbiology*, 84(22), e01185–01118.

Choi, K.-H., Kumar, A., & Schweizer, H. P. (2006). A 10-min method for preparation of highly electrocompetent *Pseudomonas aeruginosa* cells: application for DNA fragment transfer between chromosomes and plasmid transformation. *Journal of Microbiological Methods*, 64(3), 391–397.

Deatherage, D. E., & Barrick, J. E. (2014). Identification of mutations in laboratory-evolved microbes from next-generation sequencing data using breseq. In L. Sun, & W. Shou (Eds.), *Engineering and analyzing multicellular systems* (pp. 165–188). Humana Press.

Eltis, L. D., & Singh, R. (2018). *Biological funneling as a means of transforming lignin-derived aromatic compounds into value-added chemicals*. In G. T. Beckham (Ed.), *Lignin Valorization* (pp. 290-313), Royal Society of Chemistry.

Feofilova, E., & Mysyakina, I. (2016). Lignin: Chemical structure, biodegradation, and practical application (a review). *Applied Biochemistry and Microbiology*, 52(6), 573–581.

Gall, D. L., Kim, H., Lu, F., Donohue, T. J., Noguera, D. R., & Ralph, J. (2014). Stereochemical features of glutathione-dependent enzymes in the Sphingobium sp. strain SYK-6 β-aryl etherase pathway. *Journal of Biological Chemistry*, 289(12), 8656–8667.

Gellerstedt, G., & Henriksson, G. (2008). *Lignins: Major sources, structure and properties*.

Harwood, C. S., & Parales, R. E. (1996). The β-ketoadipate pathway and the biology of self-identity. *Annual Review of Microbiology*, 50(1), 553–590.

Henson, W. R., Campbell, T., DeLorenzo, D. M., Gao, Y., Berla, B., Kim, S. J., Foston, M., Moon, T. S., & Dantas, G. (2018). Multi-omic elucidation of aromatic catabolism in adaptively evolved *Rhodococcus opacus*. *Metabolic Engineering*, 49, 69–83.

Jiménez, J. I., Miñambres, B., García, J. L., & Díaz, E. (2002). Genomic analysis of the aromatic catabolic pathways from *Pseudomonas putida* KT2440. *Environmental Microbiology*, 4(12), 824–841.

Kontur, W. S., Bingman, C. A., Olmsted, C. N., Wassarman, D. R., Ulbrich, A., Gall, D. L., Smith, R. W., Yusko, L. M., Fox, B. G., Noguera, D. R., Coon, J. J., & Donohue, T. J. (2018). Novosphingobium aromaticivorans uses a Nu-class glutathione S-transferase as a glutathione lyase in breaking the β-aryl ether bond of lignin. *Journal of Biological Chemistry*, 293(14), 4955–4968.

Kuepper, J., Otto, M., Dickler, J., Behnken, S., Magnus, J., Jäger, G., Blank, L. M., & Wierckx, N. (2020). Adaptive laboratory evolution of *Pseudomonas putida* and *Corynebacterium glutamicum* to enhance anthranilate tolerance. *Microbiology*, 166(11), 1025–1037.

Kusumawardhani, H., Furtwängler, B., Blommestijn, M., Kaltenytė, A., van der Poel, J., Kolk, J., Hosseini, R., & de Winde, J. H. (2021). Adaptive laboratory evolution restores solvent tolerance in plasmid-cured *Pseudomonas putida* S12: A molecular analysis. *Applied and Environmental Microbiology*, 87(9), e00041–00021.

Li, C., Zhao, X., Wang, A., Huber, G. W., & Zhang, T. (2015). Catalytic transformation of lignin for the production of chemicals and fuels. *Chemical Reviews*, 115(21), 11559–11624.

Li, M. Z., & Elledge, S. J. (2012). SLIC: A method for sequence-and ligation-independent cloning. In *Gene synthesis* (pp. 51–59). Springer

Li, W. J., Jayakody, L. N., Franden, M. A., Wehrmann, M., Daun, T., Hauer, B., Blank, L. M., Beckham, G. T., Klebensberger, J., & Wierckx, N. (2019). Laboratory evolution reveals the metabolic and regulatory basis of ethylene glycol metabolism by *Pseudomonas putida* KT2440. *Environmental Microbiology*, 21(10), 3669–3682.

Li, W.-J., Narancic, T., Kenny, S. T., Niehoff, P.-J., O'Connor, K., Blank, L. M., & Wierckx, N. (2020). Unraveling 1, 4-butanediol metabolism in *Pseudomonas putida* KT2440. *Frontiers in Microbiology*, 11, 382.

Lim, H. G., Eng, T., Banerjee, D., Alarcon, G., Lau, A. K., Park, M.-R., & Mukhopadhyay, A. (2021). Generation of *Pseudomonas putida* KT2440 strains with efficient utilization of xylose and galactose via adaptive laboratory evolution. *ACS Sustainable Chemistry & Engineering*, 9 (34), 11512–11523.

Lim, H. G., Fong, B., Alarcon, G., Magurudeniya, H. D., Eng, T., Szubin, R., Olson, C. A., Palsson, B. O., Gladden, J. M., Simmons, B. A., Mukhopadhyay, A., Singer, S. W., & Feist, A. M. (2020). Generation of ionic liquid tolerant *Pseudomonas putida* KT2440 strains via adaptive laboratory evolution. *Green Chemistry*, 22(17), 5677–5690.

Linger, J. G., Vardon, D. R., Guarnieri, M. T., Karp, E. M., Hunsinger, G. B., Franden, M. A., Johnson, C. W., Chupka, G., Strathmann, T. J., Pienkos, P. T., & Beckham, G. T. (2014). Lignin valorization through integrated biological funneling and chemical catalysis. *Proceedings of the National Academy of Sciences*, 111(33), 12013–12018.

Malek, A. A., Chen, C., Wargo, M. J., Beattie, G. A., & Hogan, D. A. (2011). Roles of three transporters, CbcXWV, BetT1, and BetT3, in *Pseudomonas aeruginosa* choline uptake for catabolism. *Journal of Bacteriology*, 193(12), 3033–3041.

Martínez-García, E., & de Lorenzo, V. (2019). Pseudomonas putida in the quest of programmable chemistry. *Current Opinion in Biotechnology*, 59, 111–121.

Martínez-García, E., Nikel, P. I., Aparicio, T., & de Lorenzo, V. (2014). Pseudomonas 2.0: Genetic upgrading of *P. putida* KT2440 as an

enhanced host for heterologous gene expression. *Microbial Cell Factories*, 13(1), 1–15.

Meux, E., Prosper, P., Masai, E., Mulliert, G., Dumarçay, S., Morel, M., Didierjean, C., Gelhaye, E., & Favier, F. (2012). *Sphingobium* sp. SYK-6 LigG involved in lignin degradation is structurally and biochemically related to the glutathione transferase omega class. *FEBS Lett.*, 586(22), 3944–3950.

Mohamed, E. T., Werner, A. Z., Salvachúa, D., Singer, C. A., Szostkiewicz, K., Rafael Jiménez-Díaz, M., Eng, T., Radi, M. S., Simmons, B. A., Mukhopadhyay, A., Herrgård, M. J., Singer, S. W., Beckham, G. T., & Feist, A. M. (2020). Adaptive laboratory evolution of *Pseudomonas putida* KT2440 improves p-coumaric and ferulic acid catabolism and tolerance. *Metabolic Engineering Communications*, 11, e00143.

Nikel, P. I., Chavarria, M., Danchin, A., & de Lorenzo, V. (2016). From dirt to industrial applications: *Pseudomonas putida* as a synthetic biology chassis for hosting harsh biochemical reactions. *Current Opinion in Chemical Biology*, 34, 20–29.

Nikel, P. I., & de Lorenzo, V. (2018). *Pseudomonas putida* as a functional chassis for industrial biocatalysis: From native biochemistry to trans-metabolism. *Metabolic Engineering*, 50, 142–155.

Nikel, P. I., Martínez-García, E., De Lorenzo, V. (2014). Biotechnological domestication of pseudomonads using synthetic biology. *Nature Reviews Microbiology*, 12(5), 368–379.

Niu, W., Kramer, L., Mueller, J., Liu, K., & Guo, J. (2019). Metabolic engineering of *Escherichia coli* for the de novo stereospecific biosynthesis of 1, 2-propanediol through lactic acid. *Metabolic Engineering Communications*, 8, e00082.

Nogales, J., Canales, Á., Jiménez-Barbero, J., Serra, B., Pingarrón, J. M., García, J. L., & Díaz, E. (2011). Unravelling the gallic acid degradation pathway in bacteria: The gal cluster from *Pseudomonas putida*. *Molecular Microbiology*, 79(2), 359–374.

Nogales, J., García, J. L., & Díaz, E. (2017). Degradation of aromatic compounds in *Pseudomonas*: A systems biology view. *Aerobic utilization of hydrocarbons, oils and lipids*, 1–49.

Notonier, S., Werner, A. Z., Kuatsjah, E., Dumalo, L., Abraham, P. E., Hatmaker, E. A., Hoyt, C. B., Amore, A., Ramirez, K. J., Woodworth, S. P., Klingeman, D. M., Giannone, R. J., Guss, A. M., Hettich, R. L., Eltis, L. D., Johnson, C. W., & Beckham, G. T. (2021). Metabolism of syringyl lignin-derived compounds in *Pseudomonas putida* enables convergent production of 2-pyrone-4, 6-dicarboxylic acid. *Metabolic Engineering*, 65, 111–122.

Pérez, J. M. (2020). *Expanding the frontiers of plants utilization: The metabolic power of Novosphingobium aromaticivorans for lignin valorization*. The University of Wisconsin-Madison

Perez, J. M., Kontur, W. S., Alherech, M., Coplien, J., Karlen, S. D., Stahl, S. S., Donohue, T. J., & Noguera, D. R. (2019). Funneling aromatic products of chemically depolymerized lignin into 2-pyrone-4-6-dicarboxylic acid with *Novosphingobium aromaticivorans*. *Green Chemistry*, 21(6), 1340–1350.

Phaneuf, P. V., Gosting, D., Palsson, B. O., & Feist, A. M. (2019). ALEdb 1.0: A database of mutations from adaptive laboratory evolution experimentation. *Nucleic Acids Research*, 47(D1), D1164–D1171.

Ragauskas, A. J., Beckham, G. T., Biddy, M. J., Chandra, R., Chen, F., Davis, M. F., Davison, B. H., Dixon, R. A., Gilna, P., Keller, M., Langan, P., Naskar, A. K., Saddler, J. N., Tschaplinski, T. J., Tuskan, G. A., & Wyman, C. E. (2014). Lignin valorization: Improving lignin processing in the biorefinery. *Science*, 344(6185), 1246843.

Rinaldi, R., Jastrzebski, R., Clough, M. T., Ralph, J., Kennema, M., Bruijnincx, P. C., & Weckhuysen, B. M. (2016). Paving the way for lignin valorisation: Recent advances in bioengineering, biorefining and catalysis. *Angewandte Chemie International Edition*, 55(29), 8164–8215.

Salvachúa, D., Rydzak, T., Auwae, R., De Capite, A., Black, B. A., Bouvier, J. T., Cleveland, N. S., Elmore, J. R., Huenemann, J. D., Katahira, R., Michener, W. E., Peterson, D. J., Rohrer, H., Vardon, D. R., Beckham, G. T., & Guss, A. M. (2020). Metabolic engineering of

Pseudomonas putida for increased polyhydroxyalkanoate production from lignin. *Microbial Biotechnology*, 13(1), 290–298.

Sambrook, J., & Russell, D. (2000). *Molecular cloning: A laboratory manual* (3rd ed.). Cold Spring Harbor Laboratory Press.

Dos Santos, V. M., Heim, S., Moore, E., Strätz, M., & Timmis, K. (2004). Insights into the genomic basis of niche specificity of *Pseudomonas putida* KT2440. *Environmental Microbiology*, 6(12), 1264–1286.

Sato, Y., Moriuchi, H., Hishiyama, S., Otsuka, Y., Oshima, K., Kasai, D., Nakamura, M., Ohara, S., Katayama, Y., Fukuda, M., & Masai, E. (2009). Identification of three alcohol dehydrogenase genes involved in the stereospecific catabolism of arylglycerol-β-aryl ether by *Sphingobium* sp. strain SYK-6. *Applied and Environmental Microbiology*, 75(16), 5195–5201.

Schäfer, A., Tauch, A., Jäger, W., Kalinowski, J., Thierbach, G., & Pühler, A. (1994). Small mobilizable multi-purpose cloning vectors derived from the *Escherichia coli* plasmids pK18 and pK19: Selection of defined deletions in the chromosome of *Corynebacterium glutamicum*. *Gene*, 145(1), 69–73.

Schutyser, W., Renders, A. T., Van den Bosch, S., Koelewijn, S.-F., Beckham, G., & Sels, B. F. (2018). Chemicals from lignin: an interplay of lignocellulose fractionation, depolymerisation, and upgrading. *Chemical Society Reviews*, 47(3), 852–908.

Simon, R., Priefer, U., & Pühler, A. (1983). A broad host range mobilization system for in vivo genetic engineering: transposon mutagenesis in Gram negative bacteria. *Nature Biotechnology*, 1(9), 784–791.

Studier, F. W. (2005). Protein production by auto-induction in high-density shaking cultures. *Protein Expression and Purification*, 41(1), 207–234.

Sun, Z., Fridrich, B., de Santi, A., Elangovan, S., & Barta, K. (2018). Bright side of lignin depolymerization: toward new platform chemicals. *Chemical Reviews*, 118(2), 614–678.

Vrionis, H., Daugulis, A., & Kropinski, A. (2002). Identification and characterization of the AgmR regulator of *Pseudomonas putida*: Role in alcohol utilization. *Applied Microbiology and Biotechnology*, 58(4), 469–475.

Wargo, M. J. (2013). Homeostasis and catabolism of choline and glycine betaine: Lessons from *Pseudomonas aeruginosa*. *Applied and Environmental Microbiology*, 79(7), 2112–2120.

Wehrmann, M., Berthelot, C., Billard, P., & Klebensberger, J. (2019). Rare earth element (REE)-dependent growth of *Pseudomonas putida* KT2440 relies on the ABC-transporter Peda1A2BC and is influenced by iron availability. *Frontiers in Microbiology*, 10, 2494.

Willett, H. (2019). Bioproduction of adipic acid using engineered *Pseudomonas Putida* KT2440 from lignin-derived aromatics (Master's thesis, Department of Chemical and Biomolecular Engineering, University of Nebraska-Lincoln, Lincoln, Nebraska). Accessed April 28, 2022. https://digitalcommons.unl.edu/chemengtheses/40/

Zakzeski, J., Bruijnincx, P. C., Jongerius, A. L., & Weckhuysen, B. M. (2010). The catalytic valorization of lignin for the production of renewable chemicals. *Chemical Reviews*, 110(6), 3552–3599.

SUPPORTING INFORMATION

Additional supporting information can be found online in the Supporting Information section at the end of this article.